UC Davis
UC Davis Previously Published Works

Title

ER Bodies Are Induced by Pseudomonas syringae and Negatively Regulate Immunity

Permalink

Journal

ISSN

Authors

Rufián, José S
Elmore, James M
Bejarano, Eduardo R
et al.

Publication Date

DOI

Copyright Information

Peer reviewed

ER Bodies Are Induced by *Pseudomonas syringae* and Negatively Regulate Immunity

José S. Rufián[1,2,3], **James M. Elmore**[2], **Eduardo R. Bejarano**[1], **Carmen R. Beuzon**[1], **Gitta L. Coaker**[2,†]

[1]Instituto de Hortofruticultura Subtropical y Mediterránea, Universidad de Málaga-Consejo Superior de Investigaciones Científicas (IHSM-UMA-CSIC), Dept. Biología Celular, Genética y Fisiología, Campus de Teatinos, Málaga E-29071, Spain

[2]Department of Plant Pathology, University of California Davis, Davis, CA 95616, U.S.A.

[3]Shanghai Center for Plant Stress Biology, CAS Center for Excellence in Molecular Plant Sciences; Chinese Academy of Sciences, Shanghai 201602, China

Abstract

ER bodies are endoplasmic reticulum–derived organelles present in plants belonging to the Brassicales order. In *Arabidopsis thaliana*, ER bodies are ubiquitous in cotyledons and roots and are present only in certain cell types in rosette leaves. However, both wounding and jasmonic acid treatment induce the formation of ER bodies in leaves. Formation of this structure is dependent on the transcription factor *NAI1*. The main components of the ER bodies are β-glucosidases (BGLUs), enzymes that hydrolyze specialized compounds. In *Arabidopsis*, PYK10 (BGLU23) and BGLU18 are the most abundant ER body proteins. In this work, we found that ER bodies are downregulated as a consequence of the immune responses induced by bacterial flagellin perception. *Arabidopsis* mutants defective in ER body formation show enhanced responses upon flagellin perception and enhanced resistance to bacterial infections. Furthermore, the bacterial toxin coronatine induces the formation of de novo ER bodies in leaves and its virulence function is partially dependent on this structure. Finally, we show that performance of the polyphagous beet armyworm herbivore *Spodoptera exigua* increases in plants lacking ER bodies. Altogether, we provide new evidence for the role of the ER bodies in plant immune responses.

Keywords

ER bodies; plant immunity; *Pseudomonas syringae* ; *Spodoptera exigua*

ER bodies are rod-shaped endoplasmic reticulum (ER)-associated structures that are present in three families within the Brassicales order (Nakano et al. 2014). ER bodies are

---

constitutively present in roots and cotyledons of young plants (constitutive ER bodies), but their abundance decreases with senescence (Matsushima et al. 2002). In *Arabidopsis* rosette leaves, ER bodies are constitutively present in marginal cells, epidermal cells covering the midrib, and extremely large pavement cells (leaf ER bodies) (Nakazaki et al. 2019b). Furthermore, the formation of ER bodies in rosette leaves is induced by methyl jasmonate (MeJA) treatment or wounding (inducible ER bodies) (Matsushima et al. 2002).

Formation of both constitutive and leaf ER bodies is dependent on the basic helix-loop-helix transcription factor *NAI1* (Matsushima et al. 2004) and the essential protein *NAI2* (Yamada et al. 2008). Inducible ER bodies are formed in a *nai1* mutant but differ in shape and composition compared with the ER bodies induced in wild-type Col-0 (Ogasawara et al. 2009). The main components of the constitutive ER bodies are the β-glucosidases (BGLU) PYK10 (BGLU23), BGLU21, and BGLU22 (Matsushima et al. 2003), while inducible-ER bodies also contain BGLU18 (Ogasawara et al. 2009). These myrosinases belong to a subfamily of eight β-glucosidases (i.e., BGLU18 to BGLU25) (Xu et al. 2004) with ER-retention signals (Yamada et al. 2011). Leaf ER bodies mainly contain PYK10 and BGLU18 (Nakazaki et al. 2019b). PYK10 has been described as an atypical myrosinase that hydrolyzes indole glucosinolates (IG) (Nakano et al. 2017). Upon tissue damage, PYK10 associates in the cytosol with PYK10-binding protein 1 (PBP1), activating PYK10 function (Nagano et al. 2005). An *Arabidopsis pyk10/blgu18* double mutant accumulates high amounts of the IG 4-methoxyindol-3-ylmethylglucosinolate (4MI3G) after tissue damage (Nakazaki et al. 2019b). IGs and the products resulting from their breakdown have a role in defense responses against microbial pathogens and herbivory (Bednarek et al. 2009; Clay et al. 2009; Johansson et al. 2014; Millet et al. 2010; Müller et al. 2010; Nakazaki et al. 2019b). IGs are also required for the establishment of beneficial interactions with the endophytic fungus *Piriformospora indica* by appropriately regulating the level of root colonization through *PYK10* (Sherameti et al. 2008; Lahrmann et al. 2015). Collectively, multiple independent studies have supported a role in defense responses for ER bodies (Yamada et al. 2011; Nakano et al. 2014).

Plants are constantly exposed to a variety of biotic and abiotic stresses. Surface-localized plant-pattern recognition receptors (PRRs) act as one of the first lines of defense against pathogens and are able to recognize conserved pathogen features, such as flagellin, as non-self (Couto and Zipfel 2016). One of the best-characterized PRRs is the flagellin receptor FLS2 (flagellin sensing 2), which recognizes flg22, a 22–amino acid epitope of bacterial flagellin (Gómez-Gómez and Boller 2000). Perception of flg22 by FLS2 induces a number of cellular events resulting in pattern-triggered immunity (PTI), which restricts pathogen proliferation. Some of the cellular events that take place during PTI are the activation of mitogen-activated protein kinases (MAPKs) and calcium-dependent protein kinases, the production of reactive oxygen species (ROS), stomatal closure, and the formation of callose (β-1,3-glucan) deposits in the cell wall (Henry et al. 2013). However, successful pathogens have evolved different mechanisms to suppress defense responses and successfully colonize their host.

Pseudomonas syringae is a gram-negative bacterium that has been extensively used to study plant immune signaling. *P. syringae* virulence depends on the type III secretion

system (T3SS), a complex nanomachine that translocates proteins, called effectors, into the cytosol of the plant cell. Most of the effectors suppress PTI acting on different cellular pathways (Macho 2016). Another virulence mechanism used by bacterial pathogens to subvert plant immunity is the production of phytotoxins. *P. syringae* pv. *tomato* DC3000 produces coronatine, a polyketide toxin that acts as a molecular mimic of the plant hormone jasmonic acid (JA) (Weiler et al. 1994). Coronatine induces stomata reopening upon PRR perception to allow bacterial colonization (Melotto et al. 2006, 2008; Gimenez-Ibanez et al. 2017) and also suppresses callose deposition and induces bacterial growth within the apoplast (Geng et al. 2012).

In this work, we investigated the biological function of ER bodies during plant immunity. We found that ER bodies are downregulated after flg22-triggered immune activation but are induced after *P. syringae* infection in a coronatine-dependent manner. Furthermore, loci underlying ER body formation act as negative regulators of immunity against bacterial pathogens but are required for a complete response against the chewing insect *Spodoptera exigua*. With these results, we report a new role of ER bodies in virulence of phytopathogenic bacteria and their suppression by plant immune perception.

RESULTS

ER bodies are rapidly inhibited upon flagellin perception.

To investigate the role of ER body formation after plant pathogen perception, we used an *Arabidopsis* transgenic line expressing green fluorescent protein with the ER-retention signal HDEL (GFP-HDEL), which allows the visualization of ER bodies (Mitsuhashi et al. 2000). We vacuum-infiltrated 2-week-old *Arabidopsis* plants with either 100 nM flg22 or water and visualized cotyledons 3 h later by confocal microscopy. We were able to detect and quantify the ER bodies in cotyledons, in which this structure is constitutively present, in mock-treated plants. However, after flg22 treatment, only a small number of ER bodies were detected (Fig. 1A). This decrease in ER body detection was statistically different compared with water-treated controls (Fig. 1A). To further investigate the disappearance of ER bodies within the same tissue, we monitored cotyledons for 120 min after either water (mock) or flg22 treatment. ER bodies lose their characteristic rod shape within 60 min post flg22 treatment, and the GFP signal is diffused throughout the cell at later timepoints (Fig. 1B).

To analyze the impact of the flg22 treatment in ER body formation at the transcriptional level, we analyzed the transcriptional expression of *NAI1* and *PYK10* under different biotic treatments, using an available dataset (NASCArrays-120). We found that flg22 treatment reduces the expression level of *NAI1* and *PYK10* in an *FLS2*-dependent manner (Fig. 1C; Supplementary Fig. S1) (Bjornson et al. 2021), pointing to regulation of ER bodies at the transcriptional level as a consequence of activation of defense responses. However, inoculation with the virulent bacterial strain *P. syringae* pv. *tomato* DC3000 induces the expression of both *NAI1* and *PYK10* at 24 h and the same occurs with a strain expressing the avirulence effector AvrRpm1 (Fig. 1C). Interestingly, both the T3SS DC3000 mutant derivative *hrcC* and the nonhost strain 1448A reduced the accumulation of *NAI1* transcripts (Fig. 1C). Altogether, these results show a downregulation of ER bodies

as a consequence of the activation of flg22-triggered immunity and suggest a role of this subcellular structure during the defense response against *P. syringae*.

Arabidopsis mutants impacting ER body formation and contents exhibit enhanced immune responses against bacterial pathogens.

After flg22 perception, many cellular events take place to restrict pathogen invasion, including activation of MAPKs and calcium dependent protein kinases, minutes after perception, followed by ROS production, activation of defense gene expression, and, several hours later, callose deposition (Henry et al. 2013). To further characterize the role of the ER bodies in flg22-induced responses, we measured ROS production as an early event of PTI in plants affected in the formation of ER bodies. We treated 3-week-old Col-0, *nai1-1, pyk10-1*, and *pyk10-1/blgu21* plants with 100 nM flg22 and measured the ROS burst. The total ROS produced in all the mutant backgrounds tested was higher than the ROS produced in Col-0 (Fig. 2A). This increase in ROS production in response to flg22 also occurs in both *bglu18-1* and *pbp1-1* mutants (Supplementary Fig. S2A). To analyze a late event of PTI, we treated 4-week-old plants with flg22 and quantified callose deposition. Consistent with the ROS burst, the number of callose deposits was two times higher in ER body mutants compared with Col-0 (Fig. 2B). These data indicate that a loss of ER bodies or their main components induce an enhanced response to bacterial flg22, pointing to a negative role of ER bodies on PTI.

To determine the role of the ER bodies in bacterial growth, we quantified *P. syringae* pv. *tomato* DC3000 titers in Col-0 and in the different mutant backgrounds (Fig. 2C). *P. syringae* pv. *tomato* DC3000 exhibited decreased growth (>1 log) in the *nai1-1* mutant compared with Col-0. Interestingly, both the *pyk10-1* and the *pyk10-1/bglu21* mutants exhibited a stronger decrease in bacterial growth, with 1.5 log reduction compared with wild-type Col-0 (Fig. 2C). No differences were detected between *pyk10* and *pyk10-1/ bglu21*, indicating that *PYK10* is a critical gene involved in negative regulation of bacterial growth. Plants lacking *PBP1*, necessary for PYK10 function, or *BGLU18*, the main component of inducible ER bodies, also showed enhanced resistance to bacterial infection (Supplementary Fig. S2B).

A critical component controlling bacterial virulence is the ability to deliver effectors through the T3SS (Macho 2016). In order to investigate the relationship between immune suppression and ER body formation, we used DC3000 *hrcC*, which is unable to translocate effectors to the plant cell and, thus, does not suppress PTI. We measured the growth of *hrcC* in ER body mutants. In the *nai1-1* background, the growth of *hrcC* was not significantly different from that in Col-0. However, we observed a slight but significant decrease in growth in the *pyk10-1/bglu21* background (Fig. 2D). The increased *P. syringae* growth restriction in *pyk10-1*, and *pyk10-1/bglu21* backgrounds compared with *nai1* (Fig. 2C and D) could indicate a NAI1-independent regulation for one or both *PYK10* and *BGLU21*. Altogether, these results show that the absence of ER bodies increases resistance against the bacterial pathogen *P. syringae*.

NAI1 contributes to the defense response against *S. exigua.*

ER bodies have been proposed to participate in the defense response against herbivores (Nakano et al. 2014; Yamada et al. 2011). A recent study demonstrated increased susceptibility of the double mutant *bglu18 pyk10* to the terrestrial isopod *Armadillidium vulgare* (Nakazaki et al. 2019b). The *pyk10/bglu21* mutant forms ER bodies, although they are larger and less numerous than those in wild-type plants (Nagano et al. 2009). We measured the performance of the generalist leaf-chewing herbivore *S. exigua* in different ER body–related mutants. Performance assays have been widely used to study the defense mechanisms against herbivory (Chung et al. 2008; Cipollini et al. 2004; Müller et al. 2010; Santamaría et al. 2017; Van Oosten et al. 2008). We fed *S. exigua* larvae with Col-0 and the ER body mutants *nai1-1*, *pyk10-1*, and *pyk10-1/bglu21* plants and measured the weight of the larvae after 7 days. The fresh weight of *S. exigua* larvae was higher in *nai1-1* plants compared with the Col-0 control, confirming a role of ER bodies in the defense response against herbivore insects. Surprisingly, the performance of *S. exigua* in either *pyk10-1* or *pyk10-1/bglu21* plants was not different compared Col-0, suggesting a redundant role of *PYK10* and *BGLU21* with other myrosinases in this context. (Fig. 2E).

Coronatine induces the formation of ER bodies in rosette leaves.

Transcriptomic analyses indicate that inoculation with virulent *P. syringae* pv. *tomato* DC3000 induces the expression of *NAI1* and *PYK10* (Fig. 1C). To check if this increased expression results in de novo formation of ER bodies, we inoculated rosette leaves of *Arabidopsis* GFP-HDEL plants with a relatively high inoculum (5×10^7 CFU/ml) of *P. syringae* pv. *tomato* DC3000, the derivative *hrcC*, and a coronatine mutant (*cor⁻*, *P. syringae* pv. *tomato* DC3118). We applied the bacterial suspension using a brush to avoid wounding tissue. Three days after inoculation, we observed the samples under the confocal microscope (Fig. 3A). No ER bodies were found in the mock-treated leaves, in agreement with the absence of ER bodies in certain rosette leaves (Matsushima et al. 2002; Nakazaki et al. 2019b). Interestingly, a large number of ER bodies was found in leaves inoculated with wild-type *P. syringae* pv. *tomato* DC3000. The distribution of the ER bodies was patchy, suggesting that only some cells were forming the structure. To investigate if the formation of ER bodies localized surrounding bacterial colonies, we generated a *P. syringae* pv. *tomato* DC3000 derivative tagged with enhanced yellow fluorescent protein (eYFP). Three days after inoculation, we observed a large number of ER bodies surrounding the bacterial microcolony in Col-0 (Fig. 3B and C) but only a few aberrant ER bodies in the *nai1-1* mutant (Fig. 3C), suggesting that ER bodies induced by *P. syringae* pv. *tomato* DC3000 are dependent on *NAI1*. To determine which bacterial factors are inducing the formation of ER bodies in rosette leaves, we inoculated Col-0 GFP-HDEL leaves with the *hrcC* derivative and the *cor⁻* mutant, both tagged with eYFP. We were unable to detect *hrcC*–eYFP microcolonies due to their extremely small size, consistent with their reduced growth in planta. Nevertheless, we did not detect ER bodies in leaves inoculated with the *hrcC* mutant (Fig. 3A). Interestingly, the *cor⁻* eYFP mutant was unable to induce the formation of de novo ER bodies, consistent with the role of coronatine mimicking JA (Fig. 3). This result indicates that induction of ER bodies could be a virulence function of coronatine. Analyzing transcriptomic data of plants inoculated either with *P. syringae* pv. *tomato* DC3000 or the *cor⁻* mutant, we observed that many genes related to ER bodies, including *NAI1*, *PYK10*,

and *BGLU18*, were upregulated by *P. syringae* pv. *tomato* DC3000 but not after inoculation with *P. syringae* pv. *tomato* DC3118 (*cor⁻*) (Supplementary Fig. S3) (Thilmony et al. 2006). To investigate the ability of coronatine to promote bacterial virulence in the absence of wild-type ER body formation, we measured the growth of *P. syringae* pv. *tomato* DC3000 and the *P. syringae* pv. *tomato cor⁻* mutant in Col-0, *nai1-1*, *pyk10-1*, and *pyk10-1/bglu21*. In order to bypass the role of coronatine on reopening stomata (Melotto et al. 2006, 2008), we performed syringe inoculation in 5-week-old plant leaves. Four days after inoculation, a strong growth restriction was observed in the coronatine mutant compared with wild-type *P. syringae* pv. *tomato* DC3000 in Col-0 (Fig. 3D). In the ER body–defective backgrounds, a stronger growth restriction was observed for *P. syringae* pv. *tomato* DC3000 (Figs. 2C and 3D). However, the growth of the coronatine mutant was not significantly different between wild-type Col-0 and the ER body mutants.

DISCUSSION

The main contents in ER bodies are β-glucosidases, enzymes that can produce toxic compounds to protect the plant from herbivore attack (Matsushima et al. 2003). Induction of ER bodies by wounding or by MeJA treatment suggests an association with plant defense (Nakano et al. 2014). However, there is little experimental evidence of the association between ER bodies and plant immunity. Plants are infected by diverse pathogens that often utilize opposing virulence strategies and are differentially impacted by plant immune responses (e.g., chewing insects versus biotrophic or hemibiotrophic pathogens). In this study we demonstrate contrasting roles of ER bodies in the plant response to pathogenic bacteria and herbivores.

Previous studies have implicated ER bodies in plant protection against fungi and feeding insects. Sherameti et al. (2008) demonstrated that *PYK10* is required to protect plants against excessive root colonization by the endophytic fungus *Piriformospora indica*. Furthermore, Nakazaki et al. (2019b) showed that *bglu18 pyk10* double mutant plants are more susceptible than wild type to the attack of the terrestrial isopod *Armadillidium vulgare* (pillbug). In this work, we experimentally link the function of the ER bodies with the plant response against the bacterial pathogen *P. syringae* and the herbivore *S. exigua*. We found an increased weight acquisition of the generalist chewing herbivore *S. exigua* in *nai1-1* plants, compared with Col-0, but not in *pyk10-1* and *pyk10-1/bglu21* mutants (Fig. 2E). *S. exigua* feeds on leaves, in which constitutive ER bodies are absent (Matsushima et al. 2002). Constitutive leaf ER bodies, which are dependent on *NAI1*, localize in the edges of the leaves and mainly contain PYK10 and BGLU18 (Nakazaki et al. 2019b). The biogenesis and content of leaf ER bodies is regulated by both JA-dependent and -independent pathways (Nakazaki et al. 2019a). While *NAI1* expression and, therefore, PYK10 accumulation is dependent on JA, BGLU18 accumulation in leaf ER bodies is independent of JA (Nakazaki et al. 2019a). Since performance of *S. exigua* is not affected in *pyk10-1* mutants, the genetic analysis points to *BGLU18* as responsible for the defense response against *S. exigua*. Furthermore, chewing induces JA accumulation (Rehrig et al. 2014), and this signal would potentially lead to the formation of the inducible ER bodies. The *nai1* mutant is compromised in formation of inducible local and systemic ER bodies. In the *nai1* mutant, inducible ER bodies are long and tubular and mainly observed in cells

surrounding the wound site (Ogasawara et al. 2009). We also observed that *P. syringae* pv. *tomato* DC3000 was unable to induce ER body formation in the *nai1* mutant, indicating that the absence or altered composition or structure of ER bodies in *NAI1* suppresses growth of the hemibiotrophic pathogen *P. syringae*, while enhancing performance of a chewing herbivore.

P. syringae pv. *tomato* DC3000 induces the formation of ER bodies in leaves. Since the flagellin peptide flg22 downregulates the formation of constitutive ER bodies and we have shown that ER bodies negatively regulate PTI, we hypothesize that *P. syringae* induction of ER bodies is a virulence strategy to suppress host immune responses. The two main virulence factors of *P. syringae* pv. tomato are the phytotoxin coronatine and the T3SS effectors. The bacterial phytotoxin coronatine, which mimics the function of JA in the plant (Bender et al. 1999), induces the formation of ER bodies in leaves (Fig. 3A and B). JA is perceived in the plant through degradation of JASMONATE ZIM-DOMAIN (JAZ) transcriptional repressors and JAZ proteins suppress the expression of ER body components as well as indole glucosinolates (Ghorbel et al. 2021; Guo et al. 2018). Thus, JA or pathogen-JA mimics can regulate the abundance of this specialized organelle to induce or suppress defense, depending on pathogen type. The most studied coronatine virulence function is to reopen stomata upon PAMP-induced closure (Melotto et al. 2006, 2008). However, coronatine also has been shown to suppress immunity once the bacteria colonize the apoplast (Fig. 3C) (Geng et al. 2012). The T3SS defective mutant *hrcC* is not able to induce the formation of ER bodies, which would indicate an effect of T3Es on the induction of ER bodies. However, we cannot rule out that the absence of ER bodies is due to an insufficient amount of coronatine produced by the *hrcC* microcolonies.

Bacterial flg22 perception leads to a downregulation of the ER bodies at both transcriptional and posttranscriptional levels (Fig. 1; Supplementary Fig. S1). We found that *Arabidopsis* mutants defective in either ER body biogenesis or composition are more resistant to pathogenic bacteria (Fig. 2; Supplementary Fig. S2). The main components of ER bodies are myrosinases, enzymes that modify glucosinolates to initiate the glucosinolate breakdown, which will result in different products depending on the biochemical properties of the modifier protein and the chemical nature of the glucosinolate side chain (Sugiyama and Hirai 2019; Wittstock and Burow 2010). Those products can function as defense compounds or as signaling molecules.

PYK10/BGLU23 is an atypical myrosinase similar to PENETRATION 2 (PEN2, BGLU26) that hydrolyzes indole glucosinolates (IGs) (Nakano et al. 2017; Nakazaki et al. 2019b). PEN2-mediated conversion of 4MI3G into glucosinolate-derived products plays an important role in the defense response against fungi (Bednarek et al. 2009). Interestingly, *PEN2* is required for callose deposition upon flg22 perception and for resistance against *P. syringae* pv. *tomato* DC3000 infection in seedlings grown in liquid media (Clay et al. 2009; Johansson et al. 2014). In contrast, in adult plants grown in soil, callose deposition and *P. syringae* pv. *tomato* DC3000 growth is not affected in the *pen2-1* mutant (Geng et al. 2012). The *pen2-1* mutant grown in soil exhibits enhanced resistance to *P. syringae* pv. *maculicola* (Stahl et al. 2016). These apparently contradictory results indicate that PEN2 activity is dependent on one or both the age and the metabolic state of the plant. 4MI3G

overaccumulates in homogenized tissue of *bglu18/pyk10* mutants indicating that one or both of these β-glucosidases hydrolyze 4MI3G (Nakazaki et al. 2019b). Our results indicate that the single *pyk10-1* mutant and the double *pyk10-1/bglu21* mutant accumulate an increased number of callose deposits in response to flg22 treatment and are more resistant to *P. syringae* pv. *tomato* DC3000. Although both PEN2 and PYK10 seem to have the same substrate (4MI3G), their respective mutants differ on phenotypes such as flg22-induced callose deposition and resistance to *P. syringae* pv. *tomato* DC3000 (Clay et al. 2009; Johansson et al. 2014). Apart from the above-mentioned effect related to growth conditions, one of the reasons explaining these differences could be the different compartmentalization of both PEN2 and PYK10. While PEN2 is localized in peroxisome and mitochondria (Fuchs et al. 2016; Lipka et al. 2005), PYK10 localizes in ER bodies (Matsushima et al. 2003). Furthermore, myrosinase activity is regulated by different myrosinasebiding proteins and myrosinase-associated proteins as well as different specifier proteins, which lead to the formation of different breakdown products (Wittstock et al. 2016). This variety of compounds can have a direct or indirect effect on the plant defense response (Wittstock et al. 2016). It is possible that mutants lacking ER bodies or core components of ER bodies also exhibit heightened basal defense, resulting in enhanced ROS and callose production.

In conclusion, we have demonstrated the involvement of ER body–dependent regulation of immunity to bacteria and induction of ER bodies as a pathogen virulence strategy. Further work will shed light on how this novel function of ER bodies influences bacterial-plant interactions and pave the way for the discovery of the role of indole-glucosinolates breakdown on the response against bacterial invasion in plants.

MATERIALS AND METHODS

Plant material and growth conditions.

A. thaliana Col-0, the transgenic line expressing GFP-HDEL (Hayashi et al. 2001), and the mutants *nai1-1* (Matsushima et al. 2003), *pyk10-1* (Nagano et al. 2008), *pyk10-1/bglu21* (Nagano et al. 2009), *bglu18-1* (Ogasawara et al. 2009), and *pbp1-1* (Nagano et al. 2005) were grown in a controlled environment chamber at 23°C, 70% relative humidity, and a 10-h light and 14-h dark photoperiod with light intensity of 100 μE m^{-2}·s^{-1}. All seeds were stratified for 3 to 4 days at 4°C before sowing into soil.

Bacterial strains, growth conditions, and pathogen assays.

Pseudomonas syringae pv. *tomato* DC3000 (Cuppels 1986) and the derivative strains *hrcC* and *cor*$^-$ (cma$^-$ cfa$^-$ [Brooks et al. 2004]) were grown at 28°C in lysogeny broth medium (Bertani 1951). Antibiotics were used when appropriate, at the following concentrations: rifampicin, 100 μg/ml); kanamycin, 25 μg/ml; and gentamycin, 10 μg/ml.

The *P. syringae* pv. *tomato* DC3000, *hrcC*, and *cor*$^-$ eYFP derivatives were generated using a Tn*7* delivery system as previously described (Rufián et al. 2018)

For pathogen assays, 5-week-old *Arabidopsis* plants were inoculated with a *P. syringae* suspension of 5×10^4 CFU/ml prepared in 10 mM MgCl$_2$. Three leaves per plant were syringe-infiltrated and five plants were used for each experiment. Four days after

inoculation, three leaf discs of 1 cm diameter (one per leaf) were ground in 1 ml of 10 mM MgCl$_2$, and serial dilutions were plated.

Transcriptomic analyses.

For the analysis of NAI1 and PYK10 expression under different biotic stresses, we used transcriptomic data available in eFP Browser. Specifically, we used the dataset AtGenExpress: response to virulent, avirulent, T3SS-deficient, and nonhost bacteria (NASCArrays-120). Five-week-old Col-0 plants were infiltrated with the corresponding *P. syringae* strain. Samples were taken 24 h after treatment, and RNA was isolated and hybridized to the ATH1 GeneChip. The data were normalized by GCOS normalization, TGT = 100.

flg22-related assays.

For ROS burst assays, leaf discs were collected, using a cork borer of 5 mm diameter from 3-week-old *Arabidopsis* plants, and were floated overnight in deionized water. The next day, the water was replaced with an assay solution containing 17 mg of luminol per milliliter (Sigma), 10 mg of horseradish peroxidase per milliliter (Sigma), and 100 nM flg22 (Genscript). Luminescence was measured using Tristar multimode reader (Berthold Technology).

Callose deposits were quantified from 4-week-old *Arabidopsis* leaves infiltrated with a 10 μM flg22 solution. Eighteen hours after treatment, leaves were detached and incubated 15 min at 65°C in 5 ml of alcoholic lactophenol (one volume of phenol/glycerol/lactic acid/ water [1:1:1:1] and two volumes of ethanol). Leaves were transferred to fresh alcoholic lactophenol and were incubated overnight at room temperature. After two washes with 50% ethanol, leaves were stained with aniline blue and callose deposits were visualized under a fluorescence microscope. Quantification of callose deposits was performed using the Fiji distribution of ImageJ.

Confocal microscopy.

Two-week old *Arabidopsis* GFP-HDEL plants were vacuum-infiltrated with either water or 100 nM flg22. Three hours after the treatment, cotyledons were detached and observed under a Zeiss LSM710 confocal microscope equipped with an LDC-apochromat 40 × / 1.1W Korr M27 water-immersion objective (NA 1.1). GFP was excited at 488 nm and emission was collected at 500 to 550 nm. For monitoring of the dynamics of the ER bodies, cotyledons were treated as above and were visualized using a Leica SP8 confocal microscope (Leica Microsystems GmbH). GFP was excited at 488 nm and emission collected at 500 to 550 nm.

For visualization of bacterial-induced ER bodies, 5-week old *Arabidopsis* GFP-HDEL plants were brush-inoculated with a 5×10^7 CFU/ml suspension of the indicated strain (Fig. 3A). Three days after inoculation, leaves were observed as described above.

For visualization of bacterial microcolonies, 5-week old *Arabidopsis* GFP-HDEL plants were syringe-infiltrated with a 5×10^4 CFU/ml suspension and leaves were visualized using

the Leica SP5 II confocal microscope (Leica Microsystems GmbH). Images of eYFP and GFP were sequentially obtained using the following conditions (excitation/emission): eYFP (514/525 to 600 nm), GFP (488/500 to 525 nm). Z series imaging was taken at 1 μm interval. Image processing was performed using Leica LAS AF (Leica Microsystems). ER bodies were quantified using Fiji distribution of ImageJ software.

S. exigua performance.

S. exigua eggs were provided by S. Herrero (University of Valencia). After eclosion, *S. exigua* larvae were fed with an artificial diet (Elvira et al. 2010). Three days after eclosion, five larvae of approximately the same size were transferred to a 4- to 5-week-old *Arabidopsis* plant grown in Jiffy-7 pods. Larvae were transferred to new plants every 24 h to avoid food privation. Seven days after plant feeding, fresh weight of the larvae was measured. For each experiment, five replicates were performed (25 larvae per genotype).

Supplementary Material

Refer to Web version on PubMed Central for supplementary material.

ACKNOWLEDGMENTS

LITERATURE CITED

Bednarek P, Pi lewska-Bednarek M, Svatos A, Schneider B, Doubsky J, Mansurova M, Humphry M, Consonni C, Panstruga R, Sanchez-Vallet A, Molina A, and Schulze-Lefert P 2009. A glucosinolate metabolism pathway in living plant cells mediates broad-spectrum anti-fungal defense. Science 323:101–106. [PubMed: 19095900]

Bender CL, Alarcón-Chaidez F, and Gross DC 1999. *Pseudomonas syringae* phytotoxins: Mode of action, regulation, and biosynthesis by peptide and polyketide synthetases. Microbiol. Mol. Biol. Rev 63: 266–292. [PubMed: 10357851]

Bertani G 1951. Studies on lysogenesis. I. The mode of phage liberation by lysogenic *Escherichia coli*. J. Bacteriol 62:293–300. [PubMed: 14888646]

Bjornson M, Pimprikar P, Nürnberger T, and Zipfel C 2021. The transcriptional landscape of *Arabidopsis thaliana* pattern-triggered immunity. Nat. Plants 7:579–586. [PubMed: 33723429]

Brooks DM, Hernández-Guzmán G, Kloek AP, Alarcón-Chaidez F, Sreedharan A, Rangaswamy V, Peñaloza-Vázquez A, Bender CL, and Kunkel BN 2004. Identification and characterization of a well-defined series of coronatine biosynthetic mutants of *Pseudomonas syringae* pv. *tomato* DC3000. Mol. Plant-Microbe Interact 17: 162–174. [PubMed: 14964530]

Chung HS, Koo AJK, Gao X, Jayanty S, Thines B, Jones AD, and Howe GA 2008. Regulation and function of Arabidopsis *JASMONATE ZIM*-domain genes in response to wounding and herbivory. Plant Physiol. 146:952–964. [PubMed: 18223147]

Cipollini D, Enright S, Traw MB, and Bergelson J 2004. Salicylic acid inhibits jasmonic acid-induced resistance of *Arabidopsis thaliana* to *Spodoptera exigua*. Mol. Ecol 13:1643–1653. [PubMed: 15140107]

Clay NK, Adio AM, Denoux C, Jander G, and Ausubel FM 2009. Glucosinolate metabolites required for an *Arabidopsis* innate immune response. Science 323:95–101. [PubMed: 19095898]

Couto D, and Zipfel C 2016. Regulation of pattern recognition receptor signalling in plants. Nat. Rev. Immunol 16:537–552. [PubMed: 27477127]

Cuppels DA 1986. Generation and characterization of Tn*5* insertion mutations in *Pseudomonas syringae* pv. *tomato*. Appl. Environ. Microbiol 51:323–327. [PubMed: 16346988]

Elvira S, Gorría N, Muñoz D, Williams T, and Caballero P 2010. A simplified low-cost diet for rearing *Spodoptera exigua* (Lepidoptera: Noctuidae) and its effect on *S. exigua* nucleopolyhedrovirus production. J. Econ. Entomol 103:17–24. [PubMed: 20214363]

Fuchs R, Kopischke M, Klapprodt C, Hause G, Meyer AJ, Schwarzländer M, Fricker MD, and Lipka V 2016. Immobilized subpopulations of leaf epidermal mitochondria mediate PENETRATION2-dependent pathogen entry control in Arabidopsis. Plant Cell 28:130–145. [PubMed: 26721862]

Geng X, Cheng J, Gangadharan A, and Mackey D 2012. The coronatine toxin of *Pseudomonas syringae* is a multifunctional suppressor of *Arabidopsis* defense. Plant Cell 24:4763–4774. [PubMed: 23204405]

Ghorbel M, Brini F, Sharma A, and Landi M 2021. Role of jasmonic acid in plants: The molecular point of view. Plant Cell Rep. Published online.

Gimenez-Ibanez S, Boter M, Ortigosa A, García-Casado G, Chini A, Lewsey MG, Ecker JR, Ntoukakis V, and Solano R 2017. JAZ2 controls stomata dynamics during bacterial invasion. New Phytol. 213: 1378–1392. [PubMed: 28005270]

Gómez-Gómez L, and Boller T 2000. FLS2: An LRR receptor-like kinase involved in the perception of the bacterial elicitor flagellin in *Arabidopsis*. Mol. Cell 5:1003–1011. [PubMed: 10911994]

Guo Q, Yoshida Y, Major IT, Wang K, Sugimoto K, Kapali G, Havko NE, Benning C, and Howe GA 2018. JAZ repressors of metabolic defense promote growth and reproductive fitness in *Arabidopsis*. Proc. Natl. Acad. Sci. U.S.A 115:E10768–E10777. [PubMed: 30348775]

Hayashi Y, Yamada K, Shimada T, Matsushima R, Nishizawa NK, and Hara-Nishimura I 2001. A proteinase-storing body that prepares for cell death or stresses in the epidermal cells of Arabidopsis. Plant Cell Physiol. 42:894–899. [PubMed: 11577182]

Henry E, Yadeta KA, and Coaker G 2013. Recognition of bacterial plant pathogens: Local, systemic and transgenerational immunity. New Phytol. 199:908–915. [PubMed: 23909802]

Johansson ON, Fantozzi E, Fahlberg P, Nilsson AK, Buhot N, Tör M, and Andersson MX 2014. Role of the penetration-resistance genes *PEN1*, *PEN2* and *PEN3* in the hypersensitive response and race-specific resistance in *Arabidopsis thaliana*. Plant J. 79:466–476. [PubMed: 24889055]

Lahrmann U, Strehmel N, Langen G, Frerigmann H, Leson L, Ding Y, Scheel D, Herklotz S, Hilbert M, and Zuccaro A 2015. Mutualistic root endophytism is not associated with the reduction of saprotrophic traits and requires a noncompromised plant innate immunity. New Phytol. 207:841–857. [PubMed: 25919406]

Lipka V, Dittgen J, Bednarek P, Bhat R, Wiermer M, Stein M, Landtag J, Brandt W, Rosahl S, Scheel D, Llorente F, Molina A, Parker J, Somerville S, and Schulze-Lefert P 2005. Pre- and post-invasion defenses both contribute to nonhost resistance in *Arabidopsis*. Science 310:1180–1183. [PubMed: 16293760]

Macho AP 2016. Subversion of plant cellular functions by bacterial type-III effectors: Beyond suppression of immunity. New Phytol. 210:51–57. [PubMed: 26306858]

Matsushima R, Fukao Y, Nishimura M, and Hara-Nishimura I 2004. *NAI1* gene encodes a basic-helix-loop-helix-type putative transcription factor that regulates the formation of an endoplasmic reticulum-derived structure, the ER body. Plant Cell 16:1536–1549. [PubMed: 15155889]

Matsushima R, Hayashi Y, Kondo M, Shimada T, Nishimura M, and Hara-Nishimura I 2002. An endoplasmic reticulum-derived structure that is induced under stress conditions in *Arabidopsis*. Plant Physiol. 130:1807–1814. [PubMed: 12481064]

Matsushima R, Hayashi Y, Yamada K, Shimada T, Nishimura M, and Hara-Nishimura I 2003. The ER body, a novel endoplasmic reticulum-derived structure in *Arabidopsis*. Plant Cell Physiol. 44:661–666. [PubMed: 12881493]

Melotto M, Underwood W, and He SY 2008. Role of stomata in plant innate immunity and foliar bacterial diseases. Annu. Rev. Phytopathol 46:101–122. [PubMed: 18422426]

Melotto M, Underwood W, Koczan J, Nomura K, and He SY 2006. Plant stomata function in innate immunity against bacterial invasion. Cell 126:969–980. [PubMed: 16959575]

Millet YA, Danna CH, Clay NK, Songnuan W, Simon MD, Werck-Reichhart D, and Ausubel FM 2010. Innate immune responses activated in *Arabidopsis* roots by microbe-associated molecular patterns. Plant Cell 22:973–990. [PubMed: 20348432]

Mitsuhashi N, Shimada T, Mano S, Nishimura M, and Hara-Nishimura I 2000. Characterization of organelles in the vacuolar-sorting pathway by visualization with GFP in tobacco BY-2 cells. Plant Cell Physiol. 41:993–1001. [PubMed: 11100771]

Müller R, de Vos M, Sun JY, Sønderby IE, Halkier BA, Wittstock U, and Jander G 2010. Differential effects of indole and aliphatic glucosinolates on lepidopteran herbivores. J. Chem. Ecol 36:905–913. [PubMed: 20617455]

Nagano AJ, Fukao Y, Fujiwara M, Nishimura M, and Hara-Nishimura I 2008. Antagonistic jacalin-related lectins regulate the size of ER body-type beta-glucosidase complexes in Arabidopsis thaliana. Plant Cell Physiol. 49:969–980. [PubMed: 18467340]

Nagano AJ, Maekawa A, Nakano RT, Miyahara M, Higaki T, Kutsuna N, Hasezawa S, and Hara-Nishimura I 2009. Quantitative analysis of ER body morphology in an *Arabidopsis* mutant. Plant Cell Physiol. 50:2015–2022. [PubMed: 19906837]

Nagano AJ, Matsushima R, and Hara-Nishimura I 2005. Activation of an ER-body-localized beta-glucosidase via a cytosolic binding partner in damaged tissues of *Arabidopsis thaliana*. Plant Cell Physiol. 46:1140–1148. [PubMed: 15919674]

Nakano RT, Pi lewska-Bednarek M, Yamada K, Edger PP, Miyahara M, Kondo M, Böttcher C, Mori M, Nishimura M, Schulze-Lefert P, Hara-Nishimura I, and Bednarek P 2017. PYK10 myrosinase reveals a functional coordination between endoplasmic reticulum bodies and glucosinolates in *Arabidopsis thaliana*. Plant J. 89:204–220. [PubMed: 27612205]

Nakano RT, Yamada K, Bednarek P, Nishimura M, and Hara-Nishimura I 2014. ER bodies in plants of the Brassicales order: Biogenesis and association with innate immunity. Front. Plant Sci 5:73. [PubMed: 24653729]

Nakazaki A, Yamada K, Kunieda T, Sugiyama R, Hirai MY, Tamura K, Hara-Nishimura I, and Shimada T 2019b. Leaf endoplasmic reticulum bodies identified in *Arabidopsis* rosette leaves are involved in defense against herbivory. Plant Physiol. 179:1515–1524. [PubMed: 30696747]

Nakazaki A, Yamada K, Kunieda T, Tamura K, Hara-Nishimura I, and Shimada T 2019a. Biogenesis of leaf endoplasmic reticulum body is regulated by both jasmonate-dependent and independent pathways. Plant Signal. Behav 14:1622982. [PubMed: 31132914]

Ogasawara K, Yamada K, Christeller JT, Kondo M, Hatsugai N, Hara-Nishimura I, and Nishimura M 2009. Constitutive and inducible ER bodies of *Arabidopsis thaliana* accumulate distinct beta-glucosidases. Plant Cell Physiol. 50:480–488. [PubMed: 19147648]

Rehrig EM, Appel HM, Jones AD, and Schultz JC 2014. Roles for jasmonate- and ethylene-induced transcription factors in the ability of *Arabidopsis* to respond differentially to damage caused by two insect herbivores. Front. Plant Sci 5:407. [PubMed: 25191332]

Rufián JS, Macho AP, Corry DS, Mansfield JW, Ruiz-Albert J, Arnold DL, and Beuz on CR 2018. Confocal microscopy reveals in planta dynamic interactions between pathogenic, avirulent and non-pathogenic *Pseudomonas syringae* strains. Mol. Plant Pathol 19:537–551. [PubMed: 28120374]

Santamaría ME, Martinez M, Arnaiz A, Ortego F, Grbic V, and Diaz I 2017. MATI, a novel protein involved in the regulation of herbivore-associated signaling pathways. Front. Plant Sci 8:975. [PubMed: 28649257]

Sherameti I, Venus Y, Drzewiecki C, Tripathi S, Dan VM, Nitz I,Varma A, Grundler FM, and Oelmüller R 2008. PYK10, a beta-glucosidase located in the endoplasmatic reticulum, is

crucial for the beneficial interaction between *Arabidopsis thaliana* and the endophytic fungus *Piriformospora indica*. Plant J. 54:428–439. [PubMed: 18248598]

Stahl E, Bellwon P, Huber S, Schlaeppi K, Bernsdorff F, Vallat-Michel A, Mauch F, and Zeier J 2016. Regulatory and functional aspects of indolic metabolism in plant systemic acquired resistance. Mol. Plant 9:662–681. [PubMed: 26802249]

Sugiyama R, and Hirai MY 2019. Atypical myrosinase as a mediator of glucosinolate functions in plants. Front. Plant Sci 10:1008. [PubMed: 31447873]

Thilmony R, Underwood W, and He SY 2006. Genome-wide transcriptional analysis of the *Arabidopsis thaliana* interaction with the plant pathogen *Pseudomonas syringae* pv. *tomato* DC3000 and the human pathogen *Escherichia coli* O157:H7. Plant J. 46:34–53. [PubMed: 16553894]

Van Oosten VR, Bodenhausen N, Reymond P, Van Pelt JA, Van Loon LC, Dicke M, and Pieterse CMJ 2008. Differential effectiveness of microbially induced resistance against herbivorous insects in *Arabidopsis*. Mol. Plant-Microbe Interact 21:919–930. [PubMed: 18533832]

Weiler EW, Kutchan TM, Gorba T, Brodschelm W, Niesel U, and Bublitz F 1994. The *Pseudomonas* phytotoxin coronatine mimics octadecanoid signalling molecules of higher plants. FEBS Lett. 345:9–13. [PubMed: 8194607]

Wittstock U, and Burow M 2010. Glucosinolate breakdown in Arabidopsis: Mechanism, regulation and biological significance. The Arabidopsis Book 8:e0134. [PubMed: 22303260]

Wittstock U, Kurzbach E, Herfurth AM, and Stauber EJ 2016. Glucosinolate breakdown. Adv. Bot. Res 80:125–169.

Xu Z, Escamilla-Treviño L, Zeng L, Lalgondar M, Bevan D, Winkel B, Mohamed A, Cheng CL, Shih MC, Poulton J, and Esen A 2004. Functional genomic analysis of *Arabidopsis thaliana* glycoside hydrolase family 1. Plant Mol. Biol 55:343–367. [PubMed: 15604686]

Yamada K, Hara-Nishimura I, and Nishimura M 2011. Unique defense strategy by the endoplasmic reticulum body in plants. Plant Cell Physiol. 52:2039–2049. [PubMed: 22102697]

Yamada K, Nagano AJ, Nishina M, Hara-Nishimura I, and Nishimura M 2008. NAI2 is an endoplasmic reticulum body component that enables ER body formation in *Arabidopsis thaliana*. Plant Cell 20: 2529–2540. [PubMed: 18780803]
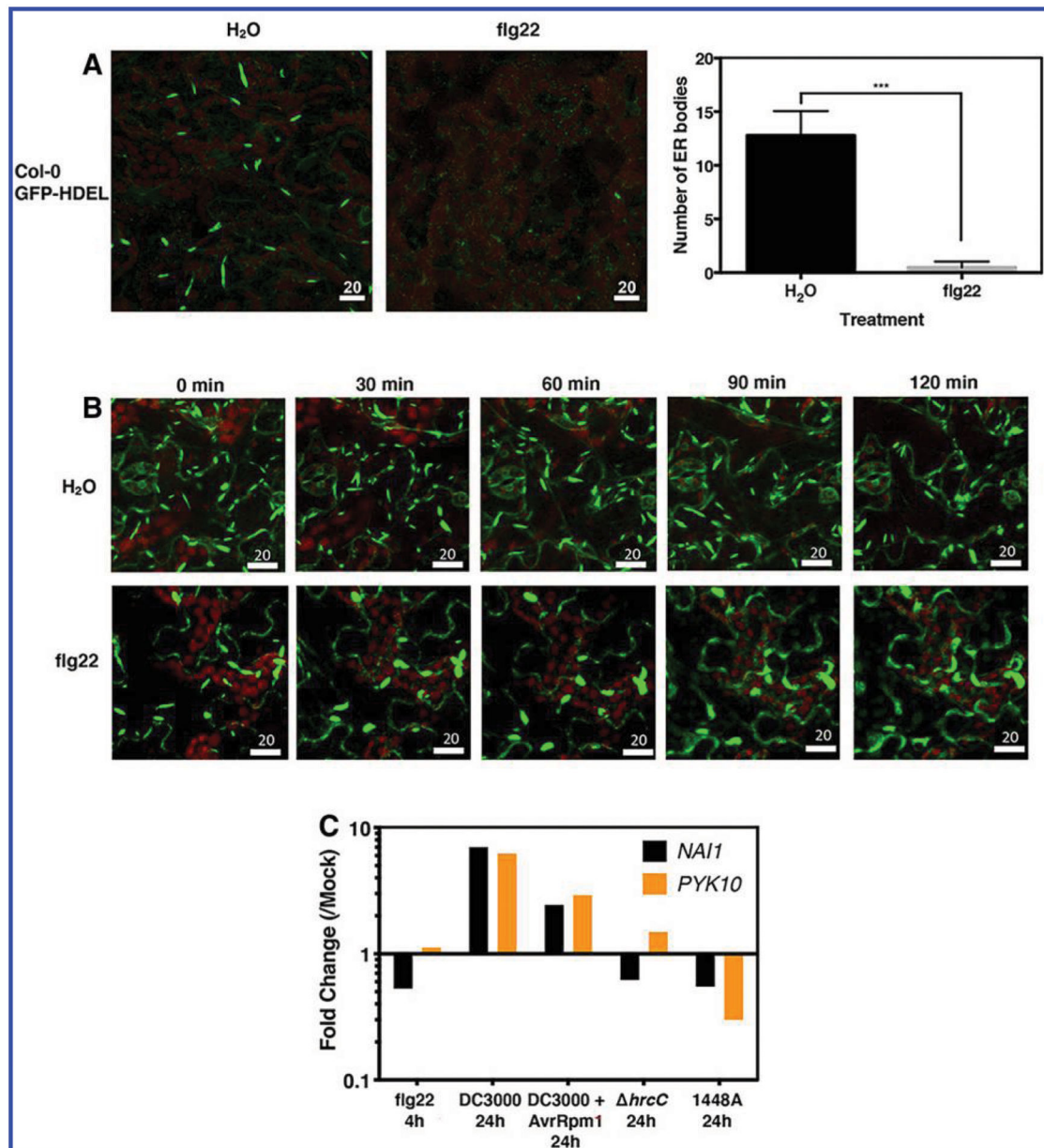
Fig. 1.

Endoplasmic reticulum (ER) bodies are downregulated after activation of pattern-triggered immunity. **A,** Constitutive ER bodies disappear after flg22 treatment. Two-week-old *Arabidopsis* plants expressing green fluorescent protein with the ER-retention signal HDEL (GFP-HDEL) were vacuum-infiltrated with water or 100 nM flg22. Cotyledons were observed in a Zeiss LSM710 confocal microscope 3 h after treatment. Red autofluorescence corresponds to chloroplasts. For ER body quantification, three fields from three independent cotyledons were used. ER bodies were quantified using Fiji. The experiment was repeated four times with similar results and a mean value ± standard error of all quantifications is shown. Statistical differences were determined with a two-tailed *t* test comparing water treatment with flg22. Three asterisks indicate $P < 0.001$. Scale bar = 20 μm. **B,** Two-week-

old *Arabidopsis* GFP-HDEL plants were vacuum infiltrated with water or 100 nM flg22. The infiltrated cotyledons were monitored for 120 min, taking photos every 5 min with a Leica SP8 confocal microscope. **C,** Expression patterns of *nai1* and *pyk10* genes under different biotic stress. Data were obtained from the available microarray in eFP Browser. Five-week-old Col-0 plant leaves were syringe-infiltrated with either a 1-μM flg22 solution (using water as mock treatment) or the indicated bacterial strain at 10^8 CFU per milliliter (using 10 mM $MgCl_2$ as mock treatment). Samples were taken 24 h after treatment. Fold change relative to mock treatment is shown.
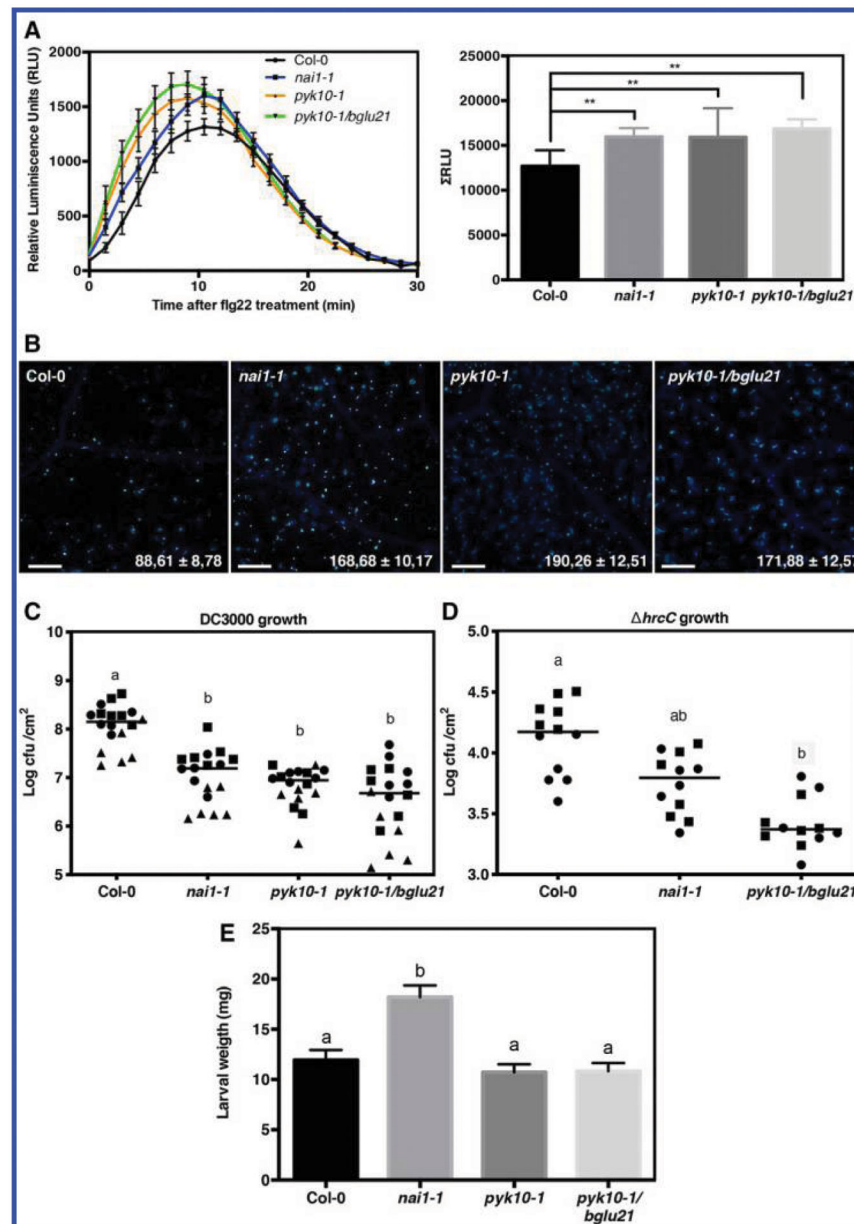
Fig. 2.
Endoplasmic reticulum body mutants exhibit enhanced immune responses and resistance against *Pseudomonas syringae*. **A,** flg22-induced reactive oxygen species (ROS) burst in Col-0, *nai1-1*, *pyk10-1*, and *pyk10-1/bglu21*. Three-week-old *Arabidopsis* leaf discs were treated with 100 nM flg22, and ROS were quantified using a luminescence based assay. The left graph represents the dynamics of the ROS produced in the different genotypes and the right graph represents the total relative light units (RLU) detected over a 30-min period. Error bars indicate standard deviation, $n = 16$. Statistically significant differences were determined with one-way analysis of variance (ANOVA) ($\alpha = 0.05$) with Tukey's multiple comparisons test, and asterisks indicate statistical significance. The experiment was repeated four times with similar results and a representative experiment is shown. **B,**

Quantification of flg22-induced callose deposition in Col-0, *nai1-1*, *pyk10-1*, and *pyk10-1/bglu21*. Four-week-old plants were infiltrated with 10 μM flg22, and callose deposits were visualized under an epifluorescence microscope 18 h after treatment. Four images were taken per leaf and nine leaves were used per experiment. The mean number of deposits was quantified and is included ± standard error (SE) in the bottom right corner of each representative image. The experiment was repeated three times with similar results, and a representative experiment is shown. White bar = 100 μm. **C,** Growth of *P. syringae* pv. *tomato* DC3000 in Col-0, *nai1-1*, *pyk10-1*, and *pyk10-1/bglu21*. Five-week-old plant leaves were syringe-inoculated with a suspension of 5×10^4 CFU/ml. Four days after inoculation, bacteria were recovered and quantified. Values from three independent replicates are shown ($n = 18$). Different symbols represent individual values from different replicates. Statistical differences were determined by ANOVA ($\alpha = 0.05$) with Tukey's multiple comparisons test, and different letters indicate statistical significance. **D,** Growth of the *P. syringae* pv. *tomato* hrcC derivative in Col-0, *nai1-1*, and *pyk10-1/bglu21*. Five-week-old plant leaves were syringe-inoculated with a suspension of 5×10^4 CFU/ml. Four days after inoculation, bacteria were recovered and quantified. Values from three independent replicates are shown ($n=18$). Different symbols represent individual values from different replicates. Statistical differences were determined by ANOVA ($\alpha = 0.05$) with Tukey's multiple comparisons test and different letters indicate statistical significance. **E,** Three-week-old *Arabidopsis* Col-0, *nai1-1*, *pyk10-1*, and *pyk10-1/bglu21* plants were challenged with 3-day-old *Spodoptera exigua* larvae. Seven days after feeding, fresh weight of each larva was measured. Bars represent the mean weight ± SE ($n=20$). Statistically significant differences were determined with one-way ANOVA ($\alpha = 0.05$) with Tukey's multiple comparisons test and different letters indicate statistical significance. The experiment was repeated three times with similar results, and a representative experiment is shown.
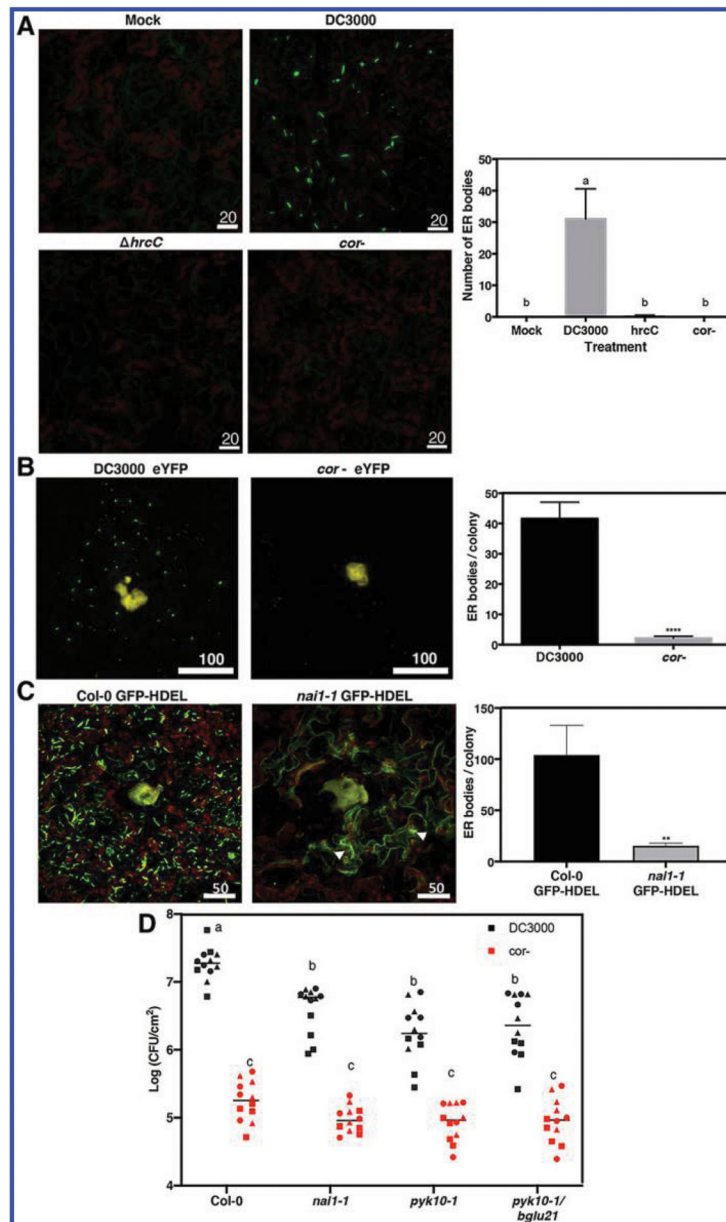
Fig. 3.

Coronatine induces formation of endoplasmic reticulum (ER) bodies in leaves and its virulence function is compromised in mutants impaired in ER body formation. **A** to **C,** Confocal microscope images of bacterial microcolonies (yellow) and ER bodies (green). Five-week-old *Arabidopsis* plants expressing green fluorescent protein with the ER-retention signal HDEL (GFP-HDEL) were brush-inoculated with a suspension containing 5×10^7 CFU/ml (A) or syringe inoculated with a bacterial suspension containing 5×10^4 CFU/ml (B and C). Three days after inoculation, leaf sections were visualized under the confocal microscope. A representative *z*-stack projection image is shown. ER bodies were quantified from the green channel using Fiji. Bars represent the mean number of ER bodies (A) or the number of ER bodies surrounding a single bacterial micro colony (B, C) ± standard

error. Red autofluorescence corresponds to chloroplasts. The experiments were repeated three times with similar results, and the mean of all experiments is shown. Statistically significant differences were determined with one-way analysis of variance (ANOVA) (α = 0.05) with Tukey's multiple comparison test (A) and different letters indicate statistical significance. Data in B and C were analyzed by t test (α = 0.001). White bar = 20 µm (A), 100 µm (B), 50 µm (C). **D,** Growth of *Pseudomonas syringae* pv. *tomato* DC3000 and its derivative coronatine mutant (*cor⁻*, DC3118) in Col-0, *nai1-1*, *pyk10-1*, and *pyk10-1/bglu21*. Five-week-old plant leaves were syringe-inoculated with a bacterial suspension of 5×10^4 CFU/ml. Four days after inoculation, bacteria were recovered and quantified. Values from three independent replicates are shown (n = 12). Different symbols represent individual values from different replicates. Statistically significant differences were determined by ANOVA (α = 0.05) with Tukey's multiple comparisons test and different letters indicate statistical significance.